NF-L in cerebrospinal fluid and serum is a biomarker of neuronal damage in an inducible mouse model of neurodegeneration

Anthony Brureau, Véronique Blanchard-Bregeon, Catherine Pech, Stéphanie Hamon, Pascal Chaillou, Jean-Claude Guillemot, Pascal Barneoud, Philippe Bertrand, Laurent Pradier, Thomas Rooney, et al.

Neurobiology of Disease 104 (2017) 73–84

Contents lists available at ScienceDirect

Neurobiology of Disease

journal homepage: www.elsevier.com/locate/ynbdi

NF-L in cerebrospinal fluid and serum is a biomarker of neuronal damage in an inducible mouse model of neurodegeneration

Anthony Brureau [a,d], Véronique Blanchard-Bregeon [b], Catherine Pech [c], Stéphanie Hamon [b], Pascal Chaillou [b], Jean-Claude Guillemot [b], Pascal Barneoud [a], Philippe Bertrand [a], Laurent Pradier [a], Thomas Rooney [a], Nathalie Schussler [a,*]

[a] Sanofi R&D, Neuroscience Research Therapeutic Area, Neurodegeneration Cluster, 1 Avenue Pierre Brossolette, Chilly Mazarin, 91380, France
[b] Sanofi R&D, Translational Sciences Unit, Chilly Mazarin, 91380, France
[c] Evotec, 19 route d'Espagne, - BP13669-31036 Toulouse Cedex 1, France
[d] Pharnext, 11 rue des Peupliers, 92130 Issy-les-Moulineaux, France

ARTICLE INFO

Article history:
Received 13 December 2016
Revised 31 March 2017
Accepted 5 April 2017
Available online 6 April 2017

Keywords:
Biomarker
Neurodegeneration
Neurofilament light chain
Cerebrospinal fluid
Inducible p25 mice

ABSTRACT

Accumulation of neurofilaments (NFs), the major constituents of the neuronal cytoskeleton, is a distinctive feature of neurological diseases and several studies have shown that soluble NFs can be detected in the cerebrospinal fluid (CSF) of patients with neurological diseases, such as multiple sclerosis and frontotemporal dementia. Here we have used an inducible transgenic mouse model of neurodegeneration, CamKII-TetOp25 mice, to evaluate whether NF-L levels in CSF or blood can be used as a biochemical biomarker of neurodegeneration. Induction of p25 transgene brain expression led to increase in CSF and serum NF-L levels that correlated with ongoing neurodegeneration. Switching off p25 prevented further increases in both CSF and serum NF-L levels and concomitantly stopped the progression of neurodegeneration. The levels of CSF NF-L detected in p25 mice are about 4–fold higher than the CSF levels detected in patients with chronic neurodegenerative diseases, such as symptomatic FTD (bvFTD). In addition, our data indicate that the NF-L detected in CSF is most likely a cleaved form of NF-L. These results suggest that CSF and serum NF-L are of interest to be further explored as potential translational dynamic biomarkers of neurodegeneration or as pharmacodynamics biomarkers at least in preclinical animal studies.

1. Introduction

Neurofilaments (NFs) are major structural elements of neurons which are present in perikarya and dendrites and particularly abundant in large myelinated axons, where they are essential for the radial growth of axons during development, the maintenance of axon caliber and the velocity of nerve conduction (Hoffman et al., 1987; Hursh, 1939; Kriz et al., 2000). NFs are heteropolymers composed of four subunits: a triplet of NF light (NF-L), NF medium (NF-M) and NF heavy (NF-H) chains and either α-internexin or peripherin in the central and peripheral nervous systems, respectively (Yuan et al., 2012). These heterodimers polymerize to form NFs which interact with cytoskeleton proteins, such as microtubules (Miyasaka et al., 1993).

Accumulation of NFs has been reported in several neurological diseases, such as in amyotrophic lateral sclerosis (ALS) where ectopic accumulation of NFs is found in the cell bodies and proximal parts of motor neurons (Corbo and Hays, 1992; Hirano, 1991). Accumulation of abnormally phosphorylated NFs has also been reported in Lewy bodies of Parkinson's disease (PD) patients (Bancher et al., 1989; Hill et al., 1993)

Abbreviations: AD, Alzheimer's disease; ALS, amyotrophic lateral sclerosis; AUROC, area under the receiver operating curve; CA1, *cornu ammonis 1*; CA3, *cornu ammonis 3*; CIS, clinical isolated syndrome; CSF, cerebrospinal fluid; Ctl mice, littermate controls (WtxHe) of p25 mice that are non-inducible mono-transgenic mice carrying only the TetO-p25 transgene; DG, dentate gyrus; FL, full-length; FTD, frontotemporal dementia; MS, multiple sclerosis; MSA, multiple system atrophy; NeuN, RNA binding protein FOX-1 homolog 3 (RBFOX3), neuronal nuclei; NF-H, neurofilament heavy chain; NF-M, neurofilament medium chain; NF-L, neurofilament light chain; NFs, neurofilaments; p25 mice, CamKII-TetOp25 mice, bitransgenic mice (HexHe), generated using the tetracycline-controlled transactivator system expressing human p25 under the control of the CamKII promoter; PD, Parkinson's disease; PSP, progressive supranuclear palsy; ROC, receiver operating curve; tTA, tetracycline-controlled transactivator system; 1 to 6wON, duration of p25 transgene induction from 1 to 6 weeks; 2wON + 3wOFF, p25 transgene induction for 2 weeks (2wON) followed by p25 transgene repression for 3 weeks (3wOFF); 3wON + 2wOFF, p25 transgene induction for 3 weeks (3wON) followed by p25 transgene repression for 2 weeks (2wOFF).

* Corresponding author at: Sanofi R&D, 1 Avenue Pierre Brossolette, 91385, Chilly Mazarin Cedex, France.
E-mail address: nathalie.schussler@sanofi.com (N. Schussler).
Available online on ScienceDirect (www.sciencedirect.com).

http://dx.doi.org/10.1016/j.nbd.2017.04.007

and in neurofibrillary tangles of Alzheimer's disease (AD) patients (Leigh et al., 1989).

Several studies have also reported that soluble NF subunits can be detected in the cerebrospinal fluid (CSF) and that increased CSF NF-L levels are associated with neuronal death and axonal degeneration in AD patients (Rosengren et al., 1996; Scherling et al., 2014; Skillbäck et al., 2014; Skillbäck et al., 2013), Parkinson-plus syndromes, such as multiple system atrophy (MSA) and progressive supranuclear palsy (PSP) (Constantinescu et al., 2010; Hall et al., 2012; Herbert et al., 2015; Holmberg et al., 1998), frontotemporal dementia (FTD) (Landqvist Waldo et al., 2013; Meeter et al., 2016; Rosengren et al., 1996; Scherling et al., 2014), Huntington's disease (Constantinescu et al., 2009), ALS and multiple sclerosis (MS) (Soelberg Sorensen and Sellebjerg, 2016). In ALS patients, an increase in CSF NF-L correlates with the conversion from bulbar/spinal to generalized ALS (Tortelli et al., 2015) and in MS an increase in CSF NFs has been shown to be a surrogate marker for neuro-axonal damage (Giovannoni and Nath, 2011). Moreover, CSF NF-L levels are elevated in patients with different stages of MS and in relapsing versus remitting forms of MS (Kuhle et al., 2013; Lycke et al., 1998; Malmestrom et al., 2003; Norgren et al., 2004; Semra et al., 2002). In addition, in patients with the relapsing form of MS, CSF NF-L levels are reduced after 6 to 12-months treatment with Natalizumab (Gunnarsson et al., 2011). Taken together, these data suggest that increased CSF NF-L levels could be a biomarker of the neurodegenerative process that could be used to stratify patients and to monitor the progression of neurodegeneration and the efficacy of neuroprotective therapies.

NF-L has also been detected in human blood using a highly sensitive electrochemiluminescent assay (Gaiottino et al., 2013; Limberg et al., 2016) or SIMOA technology (Rohrer et al., 2016; Rojas et al., 2016). Serum NF-L has been shown to be increased in clinical isolated syndrome (CIS) (Disanto et al., 2015) and in early relapsing remitting MS where it correlates with NF-L levels in CSF (Kuhle et al., 2016). Moreover, serum NF-L can discriminate between ALS and healthy controls (Gaiottino et al., 2013; Lu et al., 2015), differentiate PD from atypical PD (Hansson et al., 2017), predict disease progression in PSP (Rojas et al., 2016) and be used as a prognostic biomarker for the clinical onset and severity in FTD (Meeter et al., 2016). A strong correlation between serum NF-L and CSF NF-L levels has also been reported (Rojas et al., 2016; Meeter et al., 2016; Hansson et al., 2017).

In another recent publication (Bacioglu et al., 2016), CSF and blood levels of NF-L were also evaluated in murine models of alpha-synucleinopathies, tauopathy, and β-amyloidosis and were reported to be increased in conjunction with the appearance of proteopathic lesions and axonal pathology.

In the present study, we have evaluated whether NF-L levels in CSF or blood can be used as a biomarker of neurodegeneration in an inducible transgenic mouse model of neurodegeneration, the CamKII-TetOp25 model (referred to as p25 mice) (Cruz et al., 2003). In this model, prolonged p25 expression causes severe synaptic and neuronal loss and brain atrophy which are accompanied by cognitive deficits (Cruz et al., 2003; Fischer et al., 2005). Repression of p25 transgene expression stops global brain atrophy, neuronal loss and astrogliosis, suggesting that the pathogenesis in this model can be regulated by switching on and off p25 expression (Fischer et al., 2005). We have used the ability to induce and switch off neurodegeneration in p25 mice to evaluate the kinetic profile of NF-L levels in CSF and serum. Our data demonstrate that increased levels of NF-L in the CSF and blood correlate with induced neuronal damage in the cortex and hippocampus of p25 mice and that the NF-L measured in the CSF is probably a cleaved form of NF-L.

2. Material and methods

2.1. Animals

All mice in this study were produced and provided by Charles River (France). Experiments were performed in our AAALAC-accredited facility in full compliance with standards for the care and use of laboratory animals, according to French and European Community (Directive 2010/63/EU) legislation. All procedures were approved by the local Animal Ethics Committee (CEEA #24) and the French Ministry for Research. Mice were housed in a pathogen-free facility, one per cage, and maintained on a 12-h light/dark cycle with ad libitum access to food and water.

CamKII-TetOp25 mice (p25 mice) were generated, as described by Cruz et al. (2003). Briefly, p25 bitransgenic mice were generated using the tetracycline-controlled transactivator system to express human p25 under the control of a CamKII promoter, which drives high p25 transgene expression in the forebrain. In the presence of the tetracycline derivative, doxycycline, expression of the p25 transgene is repressed. All the mice in this study, including littermate controls, were exposed to doxycycline in utero and maintained on a doxycycline containing diet until 6 weeks of age, at which point doxycycline was removed from their diet to induce expression of the p25 transgene. This event is, hereafter, referred to as "induction". He × He genotype refers to bitransgenic animals (p25 mice), whereas Wt × He genotype corresponds to littermate controls (control mice) that are non-inducible mono-transgenic mice carrying only the TetO-p25 transgene. The very low level of p25 expression in control mice is similar to the level of p25 detected in non-induced p25 mice (data not shown).

2.2. Study design parameters

Both male and female mice were used in this study. There were no a priori specific exclusion criteria, other than animal health and ethical standards. The numbers of mice per group were based on the size of the animal batches and on preliminary data, but no power calculation or sample size determination was performed. No statistical randomization schedule was used, but induction start (removal of doxycycline from diet), biofluids and tissue sampling was organized so that, at the end of the experiment, samples from each group were equally distributed during sampling.

2.3. CSF and blood sampling

Animals were anesthetized with an intraperitoneal injection of a mixture of ketamine hydrochloride (50 mg/kg) and xylazine (10 mg/kg). CSF was sampled, as previously described (DeMattos et al., 2002). Briefly, animals were placed on a platform and the arachnoid membrane covering the cisterna magna was punctured. The positive flow pressure allows collection of CSF using a micropipette with a narrow tip. Five to twenty microliters of CSF per mouse were collected and stored at −80 °C in polypropylene tubes. The animals were then removed from the platform and an intracardiac blood puncture performed. Blood was collected in a microvette 500-Z gel® (Sarstedt) containing a clotting activator for serum isolation. The microtubes were centrifuged for 5 min at 10,000 × *g* and sera were collected and stored at −80 °C.

2.4. Brain sampling

Brains were dissected out and one hemi-brain was kept for Western blot analysis and the other was prepared for immunohistochemistry. For Western blot analysis, cerebral cortices were quickly frozen in cooled isopentane and then stored at −80 °C. The hemi-brain used for immunohistochemistry was immersion-fixed in 4% formaldehyde for 7 days. Post-fixed hemi-brains were rinsed in phosphate-buffered saline (PBS) and cryoprotected in a 20% sucrose solution and then frozen. Serial sagittal cryostat (Microm, HM560) sections were collected onto microscope glass slides (Flex, Dako) and then stored at −20 °C, or placed in PBS-sodium azide 0.1% containing wells and stored at 4 °C.

2.5. Histology and immunohistochemistry

Fluoro-Jade B histology was performed using an anionic fluorescein derivative dye as a marker of cells undergoing degeneration (Schmued et al., 1997). For this purpose, 14 μm cryostat sections were directly mounted onto slides (Flex, Dako). The slides were first rehydrated in distilled water and then transferred to a solution of 0.06% potassium permanganate for 30 min under gentle agitation on a rotating platform. The slides were then rinsed and incubated in a 0.0004% Fluoro-Jade B solution prepared in 0.1% acetic acid (AG310, Chemicon). Slides were then rinsed and rapidly air-dried on a slide warmer (50 °C). Finally, the slides were cleared by immersion in xylene for at least 1 min before coverslipping with Eukitt mounting media.

Immunohistochemistry of RNA binding protein FOX-1 homolog 3 (RBFOX3), also known as neuronal nuclei (NeuN), was performed on 20 μm free-floating sections. NeuN is an RNA-binding protein localized in the nucleus and in the cytoplasm that regulates alternative splicing events, and is used as a sensitive and specific neuronal marker (Kim et al., 2009; Wolf et al., 1996). Briefly, sections were washed in 0.1 M PBS/0.15% Triton X-100 solution and incubated in 0.3% hydrogen peroxide at room temperature for 30 min. They were further incubated for 30 min in blocking buffer, 0.01 M PBS/10% BSA, and then overnight in primary antibody solution (NeuN mouse monoclonal antibody, MAB377B, Millipore Chemicon International) diluted at 1/100. After successive incubations with a secondary goat anti-mouse immunoglobulin antibody (BA9200, Vector Laboratories) and peroxidase-coupled avidin complex (Vectastain ABC kit, Vector Laboratories) diluted at 1/400, sections were developed in a substrate solution of 0.05% diaminobenzidine tetrahydrochloride and 0.003% hydrogen peroxide in PBS 0.1 M. They were then rinsed in 0.1 M PBS and mounted on slides.

2.6. Quantitative image analysis

Quantitative analysis of Fluoro-Jade B and NeuN staining was based on virtual microscopic slide technology, including the use of a slide scanner system (Olympus Dotslide system) equipped with a BX51 microscope with fluorescent applications and a computer-based workstation (Explora Nova using Mercator software). For both markers, five high-resolution brightfield or fluorescent (FITC filter) images, that included dorsal parts of the hippocampal and surrounding cortical areas, were taken at different positions along the sagittal lateromedial axis of the hemi-brain and analysed for each animal. Manual counting of Fluoro-Jade B-positive cells and measurement of the optical density of NeuN immuno-staining (used as an index of neuronal cell density) were performed in fixed subareas of the dentate gyrus, CA1 and CA3, and cortical layers II and VI using Mercator image analysis software (ExploraNova, France). Multiple sections were pooled within each animal to yield a mean value of Fluoro-Jade B-positive cell count or NeuN staining optical density for each analysed brain region. These values were used to calculate the medians ± interquartile range in a given group. Although the slides were coded, the observer was not blind to experimental groups when performing quantitative analyses. Data and metadata traceability was ensured by the equipment which automatically loads and links bar-coded meta-data with the resulting virtual image.

2.7. NF-L ELISA assay

The sandwich ELISA NF-light® assay (UmanDiagnostics, Umeå, Sweden) used contains two highly specific NF-L monoclonal antibodies targeting the rod region of NF-L, with no cross-reactivity with other known brain antigens: capture monoclonal antibody 47:3 and biotinylated detector monoclonal antibody 2:1 (Norgren et al., 2002; Norgren et al., 2003). The ELISA was run as described in the NF-light® assay instructions, with the following adaptation: CSF samples (5–20 μL) were diluted in a final volume of 100 μL. For sera, 50 μL was assayed in a final volume of 100 μL. Due to the small volumes of CSF samples and in order to avoid variability across plates, all samples from a given study were randomized and run on a single ELISA plate. The absorbance was read at 450 nm with a VersaMax microplate reader (Molecular Devices). A 4-parameter logistic regression was performed to provide the best curve fit using Softmax® Pro software. Results are expressed as ng/L of CSF or serum. The detection level of the assay was around 1.5 pg/well (corresponding to 31 ng/L when 50 μL was assayed).

Spike recovery in human CSF has already been documented (see Instructions for Use version 2016/04 from NF-light® assay), with recovery yield of 88–99% in the interval 250–2500 ng/L. We also performed spike recovery testing in Wt mouse serum: following addition of known amounts of NF-L to 50 μL of serum per well, the recovery yield was 62–70% in the interval 1000–5000 ng/L (Supplementary data, Fig. S1).

2.8. Western blot

2.8.1. Evaluation of p25-GFP protein expression in cerebral cortex

Tissues were lysed in RIPA buffer (Cell Signaling), containing protease and phosphatase inhibitors (ThermoScientific), in Precellys tubes (CK14). After lysis, samples were centrifuged at 14,000 × *g* for 10 min at 4 °C and the supernatants stored at −80 °C.

Protein concentration was determined using DC Protein® Assay (Biorad). Equal amounts of total proteins were submitted to Western blot analysis with the Novex® NuPAGE® gel electrophoresis system, according to manufacturer's instructions (Life Technologies). Proteins were denatured in LDS buffer containing DTT and then loaded onto a NuPAGE® 4–12% Bis-Tris Mini gel to perform the electrophoresis. Proteins were then transferred to polyvinylidene difluoridine (PVDF) membranes (0.45 μm, Life Technologies). Membranes were blocked with TBS/Tween 20 0.1%/BSA 5% and incubated overnight at 4 °C with a rabbit polyclonal primary antibody raised against the C-terminal of p35 (C-19) (Santa Cruz) followed by an incubation with an anti-rabbit IgG HRP-conjugated secondary antibody (GE Healthcare) for 1 h at room temperature in TBS/Tween 20 0.1%/milk 5%. Immuno-reactive proteins were revealed using an electrochemiluminescence detection kit (GE Healthcare). The electrochemiluminescent signal was captured with a high-resolution CCD camera LAS-3000 (Fujifilm) and densitometry measured with MultiGauge software. To allow quantification across several gels, one sample was used as an internal calibrator and was loaded on each gel and set to 100%.

2.8.2. Evaluation of CSF NF-L

To enrich samples in NF-L before Western blot evaluation and to eliminate high amounts of albumin, which migrates very close to NF-L (data not shown), CSF NF-L or recombinant bovine NF-L was first immuno-captured by incubating samples for 1 h in the ELISA plate from the NF-light® assay which is coated with an antibody against-NF-L (capture monoclonal antibody 47:3). Then, after washing, 25 μL of boiled LDS buffer containing DTT was added to the wells for 10 min at 70 °C. Denatured samples containing the immuno-captured NF-L were then subjected to SDS-PAGE analysis. NF-L proteins were revealed using a rabbit monoclonal antibody raised against NF-L as a primary antibody (Cell Signaling, C28E10) and an anti-rabbit IgG HRP-conjugated as a secondary antibody (GE Healthcare).

2.9. Statistics

Statistical analyses were conducted using SAS 9.2 (SAS Institute Inc., Cary, NC, USA), and graphs were generated using GraphPad Prism® version 5 for Windows (GraphPad Software, San Diego, CA, USA).

2.9.1. ON study

In the exploratory ON study (Fig. 1) data from 11 control (Ctl = Wt × He, 4 males and 7 females) and 42 p25 mice (He × He, 15 males and 27 females) were analysed. Statistical analysis was performed to

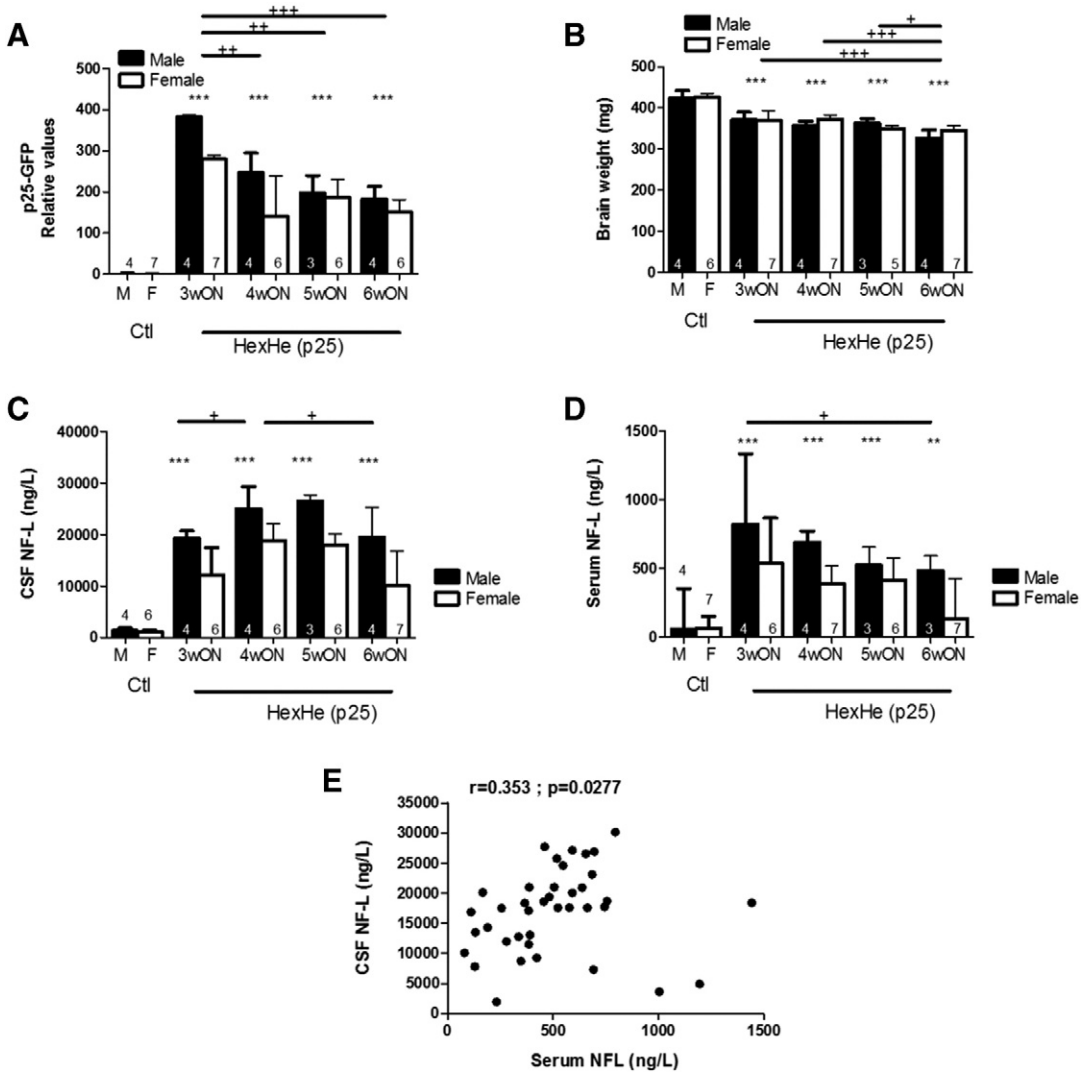

Fig. 1. CSF and serum NF-L levels increase upon p25 transgene induction. (A) Quantification of p25-GFP fusion protein expression in cortex after 3, 4, 5 and 6 weeks of p25 transgene induction, as measured by Western blot. p25-GFP expression in 3wON group was significantly different from all other groups of induced p25 mice (4, 5 and 6wON), both sexes included. (B) Measurement of brain weights after 3, 4, 5 and 6 weeks of p25 transgene induction. Brain weights in 6wON group were significantly different from all other groups (3, 4 and 5wON), both sexes included. (C) CSF NF-L levels after 3, 4, 5 and 6 weeks of p25 transgene induction. CSF NF-L levels at 4wON were significantly different compared to 3wON and 6wON, both sexes included. (D) Serum NF-L levels after 3, 4, 5 and 6 weeks of p25 transgene induction. Serum NF-L levels at 6wON were significantly different compared to 3wON, both sexes included. For Fig. 1A to D, histograms are represented as medians + interquartile range except for brain weights (means + sem). Black bars represent male p25 mice and white bars represent female p25 mice. The number of animals in each group is indicated within the columns of histograms. Statistical analyses were performed on rank-transformed data, except for brain weights (raw data). Effect of transgene induction: Two-tailed Dunnett's test versus Ctl group $^{*}p < 0.05$, $^{**}p < 0.01$, and $^{***}p < 0.001$. Effect of duration of transgene induction: Two-way analysis of variance in induced p25 revealed a significant group and sex effect, except for brain weights for which no sex effect was evidenced. Winer analysis was then performed followed by a Newman-Keuls test on rank-transformed data, except for brain weights (raw data) $+p < 0.05$, $++p < 0.01$ and $+++p < 0.001$. (E) Correlation between CSF and serum NF-L levels in induced p25 mice (Ctl animals were excluded from the analysis). A Spearman coefficient of correlation was calculated ($r = 0.352$; $p = 0.0277$; $n = 39$ animals).

evaluate the effect of p25 transgene induction compared to Ctl mice or the effect of the duration of p25 induction. Further details on statistical analysis are provided in Supplementary methods.

2.9.2. ON-OFF study

In the ON-OFF study (Figs. 2, 3 and 4), data from 12 Ctl (6 males and 6 females) and 60 p25 mice (30 males and 30 females) were analysed; 1 animal died before CSF sampling. The effect of the duration of p25 transgene induction and the impact of switching off p25 transgene expression were analysed in p25 male mice only. Further details on statistical analysis are provided in Supplementary methods.

In addition, Spearman correlation coefficients were calculated between the parameter "CSF NF-L" and the parameters "brain weight", "p25-GFP", "serum NF-L", "NeuN" and "Fluoro-Jade B", respectively. Spearman correlation coefficients were also calculated between the parameter "Serum NF-L" and the parameters "NeuN" and "Fluoro-Jade B".

2.9.3. ROC curves

Receptor operating characteristic (ROC) curve analysis of CSF and serum NF-L levels were analysed according to Robin et al. (2011). Further details on statistical analysis and optimal threshold determination are provided in Supplementary methods.

3. Results

3.1. CSF and serum NF-L levels increase upon p25 transgene induction

We first assessed the effect of different time periods of p25 transgene induction (ON) on p25-GFP protein levels in the cerebral cortex. Fig. 1A shows that p25-GFP protein was maximally expressed after 3 weeks of p25 transgene induction (3wON) in both male and female mice, with higher levels in male mice, and then progressively

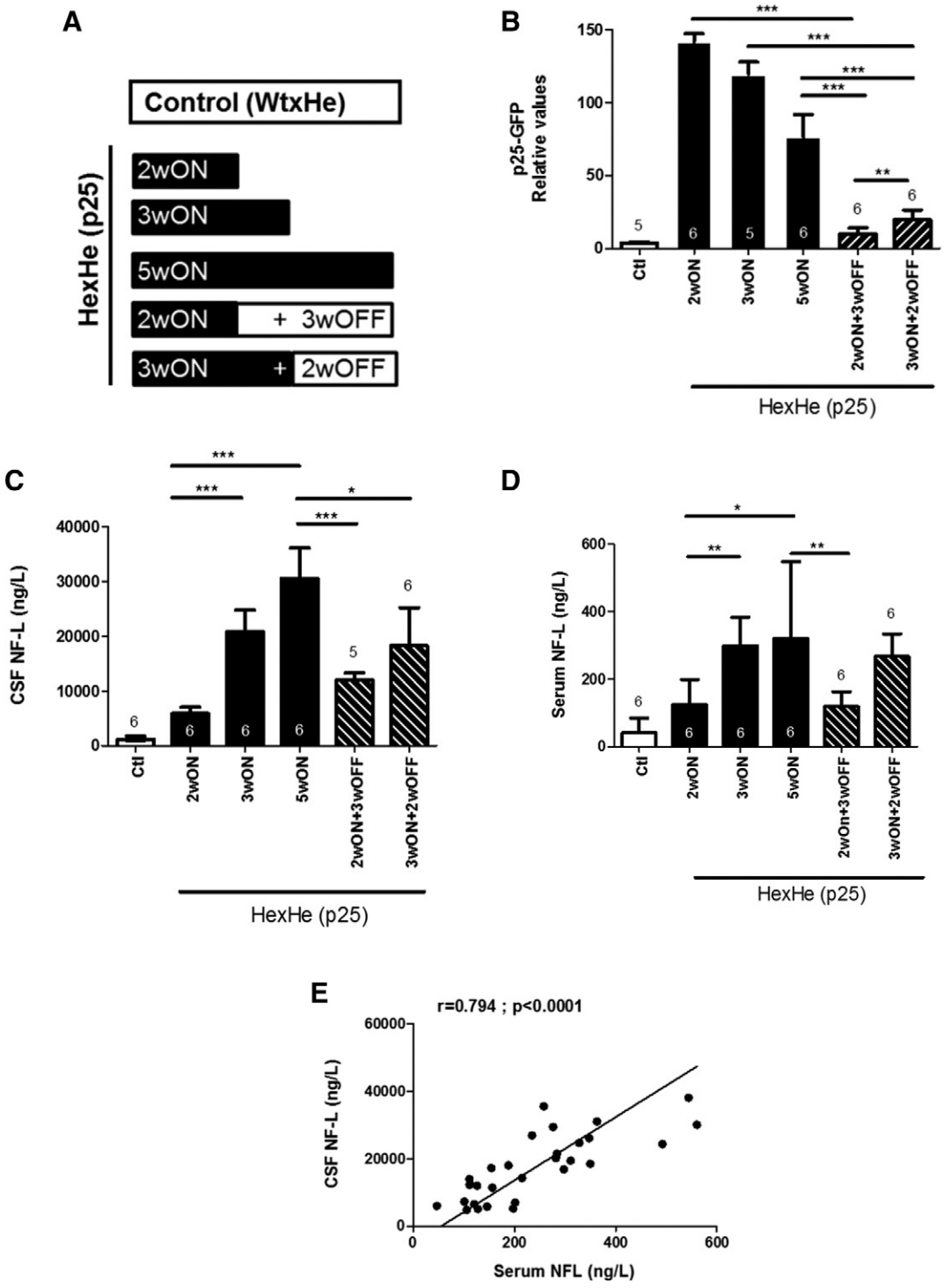

Fig. 2. Increase in CSF and serum NF-L levels is blocked when p25 transgene is repressed. (A) Experimental design of p25 transgene induction and repression (ON-OFF study). (B) Quantification of p25-GFP fusion protein expression in the cerebral cortex upon transgene induction (2, 3 and 5wON) and repression (2wON + 3wOFF and 3wON + 2wOFF), as measured by Western blot. (C) CSF NF-L levels upon transgene induction and repression. (D) Serum NF-L levels upon transgene induction and repression. For Fig. 2B to D, results are expressed as medians + interquartile range. The number of animals (male mice only) in each group is indicated within the columns of the histograms. A one-way analysis of variance followed by a Newman-Keuls test was performed on rank-transformed data to compare different groups of p25 male mice; *$p < 0.05$, **$p < 0.01$, and ***$p < 0.001$. (E) Correlation analysis between CSF and serum NF-L levels in male mice (Ctl mice were excluded from the analysis). Spearman rank correlation analysis ($r = 0.794$, $p < 0.0001$) and Deming linear regression line.

declined with robust expression still detected after 6 weeks of induction. As previously reported by Cruz et al. (2003), induction of p25 induced a significant brain atrophy as revealed by the decrease (−13%) in brain weights in both male and female p25 mice after 3 weeks of p25 transgene induction (Fig. 1B). Brain atrophy increased with induction duration (reduction of brain weights of −23% and −19% after 6 weeks of induction in male and female p25 mice, respectively). This increase in brain atrophy probably explains, at least in part, the decrease of p25 protein expression in the cortex.

CSF NF-L levels were significantly increased following induction of p25 at all-time points tested, with CSF NF-L levels being higher in

male mice than in female mice (Fig. 1C, sex effect: $p < 0.0001$). The highest CSF NF-L levels were reached after 4 weeks of induction in female (4wON: 18,862 ng/L) and after 5 weeks of induction in males (5wON: 26,530 ng/L in male mice) (Fig. 1C). At 6wON, there was a decrease of CSF NF-L levels to 10,071 ng/L (−47%) and 19,478 ng/L (−27%) in female and male mice, respectively (global significant difference, all animals included, observed between 4 and 6wON: $p = 0.0355$). In two separate experiments on female mice, after 10 weeks of induction, CSF NF-L was also significantly reduced (−58% and −46%) in comparison to 5wON (data not shown).

No significant correlation was found between CSF NF-L levels and p25-GFP protein levels in the cerebral cortex ($r = 0.224$, $p = 0.1764$), suggesting that the increase of NF-L levels is not directly linked to p25 transgene expression, but is a secondary consequence of mechanism(s) induced by p25 overexpression (i.e., neuronal death of p25 expressing neurons or synaptic loss). There was also no significant correlation between brain weights and CSF NF-L levels ($r = -0.198$, $p = 0.2267$).

The concentrations of serum NF-L, which were at least 20-fold lower than CSF NF-L levels, also increased in p25 mice after p25 transgene induction (Fig. 1D) but did not change between 3 and 5wON. The increase in serum and CSF NF-L levels were significantly correlated ($r = 0.353$, $p = 0.0277$, Fig. 1E). Three animals appear to be outside of the correlation scatter plot. These mice (1 female and 2 male) were in the 3wON group and showed higher serum NF-L levels (>1000 ng/L) in comparison to all other mice. Such high serum NF-L levels should be taken with caution since they were not confirmed in the following ON-OFF study.

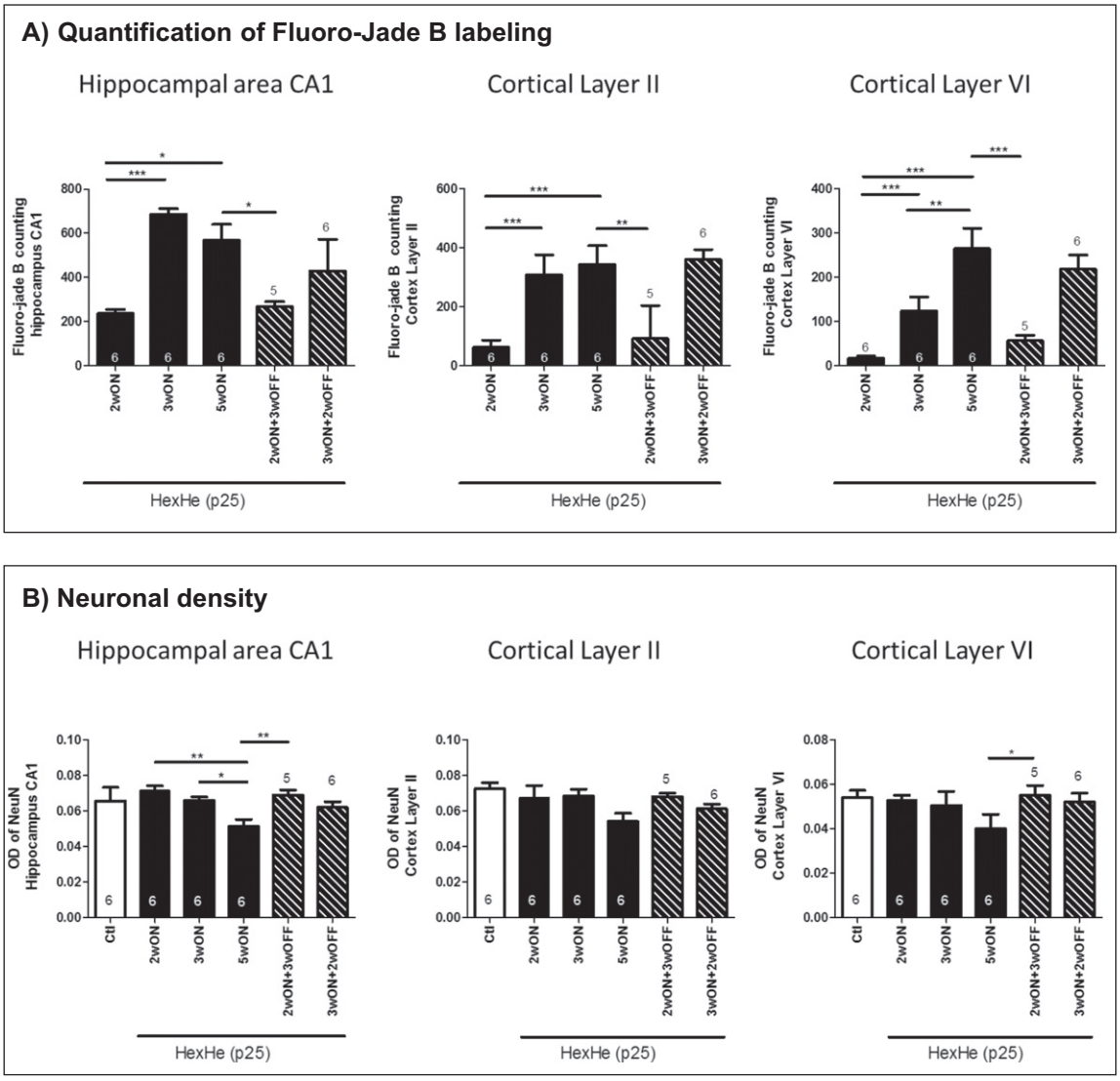

Fig. 3. Ongoing neurodegeneration (Fluoro-Jade B) and neuronal loss (NeuN) is blocked when p25 transgene expression is switched off. (A) Quantification of Fluoro-Jade B-positive cell number upon p25 transgene induction in male mice in CA1 hippocampal area and cerebral cortical layers II and VI. (B) Measurement of neuronal density (optical density of NeuN positive signal) upon p25 transgene induction in male mice in CA1 hippocampal area and cerebral cortical layers II and VI. Results are expressed as medians + interquartile range. The number of animals (male mice only) in each group is indicated within the columns of histograms. A one-way analysis of variance followed by a Newman-Keuls test on rank-transformed data was performed to compare all groups of p25 male mice; $^{*}p < 0.05$, $^{**}p < 0.01$ and $^{***}p < 0.001$. (C) High-resolution fluorescent (FITC filter) photomicrographs (×10 magnification) illustrating distribution and density of Fluoro-Jade B-positive cells in dorsal hippocampus (a, b, c) and cortex (a′, b′, c′). Sections were selected in middle part of the hemi-brain of one representative male p25 mice (He × He) from the 2wON (a), 5wON (b) and 2wON + 3wOFF (c) groups. On images a, b and c, white arrows indicate neuronal injury extent in CA1 hippocampal area. On images a′, b′ and c′, one or two white asterisks indicate ongoing neurodegeneration in cortical layers II or VI respectively. Of note, no Fluoro-Jade B-positive cells were detectable in control mice (Wt × He) (data not shown). Scale bars = 200 μm. (D) High-resolution bright-field photomicrographs (×10 magnification) illustrating the density of NeuN-positive neurons in entire sagittal section selected in middle part of the hemi-brain of one representative male control mice (a) and p25 mice from the 5wON (b) and 2wON + 3wOFF (c) groups. Inserts a′, b′, c′ focused on cortical layers II or VI (delimited in the top and bottom of the cortical structure respectively) and hippocampal CA1 in bottom of images (black arrow). Scale bars = 1 mm and 100 μm for top and bottom panels, respectively.

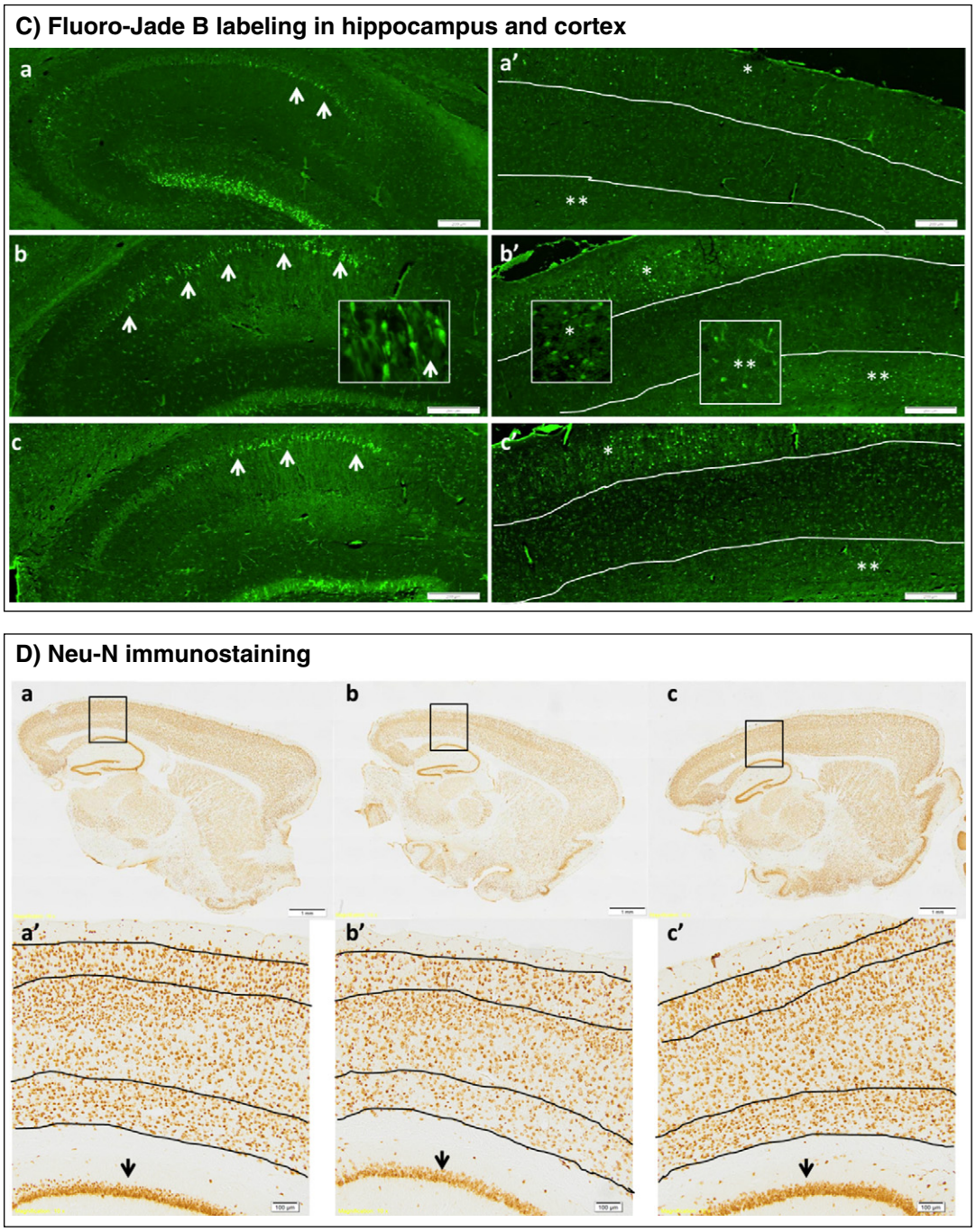

Fig. 3 (*continued*).

3.2. The increase in CSF NF-L levels is stopped when p25 transgene is switched off

To evaluate the sensitivity of CSF NF-L levels to p25 expression, p25 transgene expression was switched off after 2 or 3 weeks of p25 induction for a period of 3 or 2 weeks (2wON + 3wOFF and 3wON + 2wOFF, respectively) (Fig. 2A). Since both p25-GFP protein expression and CSF NF-L levels were consistently higher in male mice than in female mice (Fig. 1A), separate experiments were performed with only male (Fig. 2B and C) or female mice (Supplementary data, Fig. S2A and B).

The overexpression of p25-GFP in the cerebral cortex was almost completely abolished when p25 transgene was switched off (Fig. 2B) with the residual expression of p25-GFP being higher in the 3wON + 2wOFF group than in the 2wON + 3wOFF group ($p = 0.0011$), suggesting that transgene turnover was ongoing but still incomplete after 2 weeks of transgene repression. The increase in CSF NF-L levels was also stopped when p25 expression was switched off (Fig. 2C). CSF NF-L levels in animals in which p25 expression was switched off after 2 weeks of induction (2wON + 3wOFF: 11,958 ng/L) or 3 weeks of induction (3wON + 2wOFF: 18,262 ng/L) were significantly lower ($p < 0.0001$ and $p = 0.0213$, respectively) than those in animals where p25 expression was induced for 5 weeks without switching off p25 expression (5wON: 30,554 ng/L). Moreover, CSF NF-L levels in both groups did not return to the basal levels measured in control mice (1136 ng/L), and did not significantly differ from CSF NF-L levels measured in animals before the onset of p25 gene repression

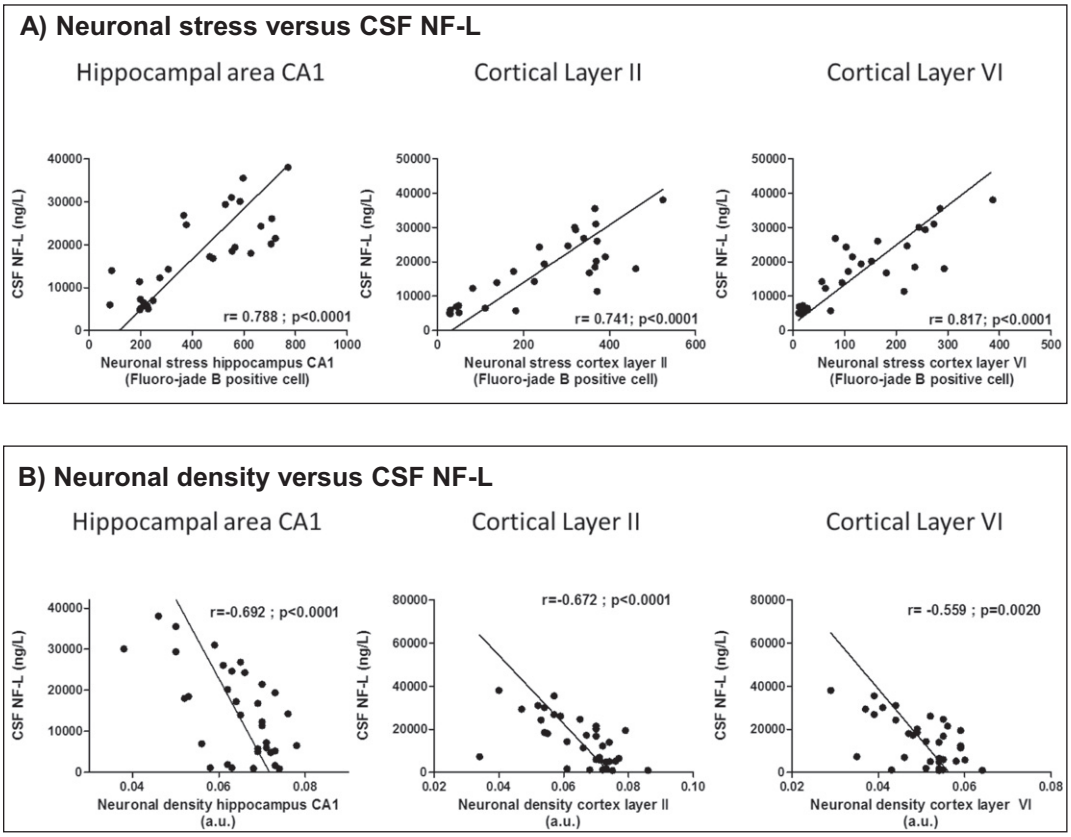

Fig. 4. Correlation between CSF NF-L levels and neuronal damage in brain of p25 mice. (A) Correlation between ongoing neurodegeneration (number of Fluoro-Jade B-positive cells) and CSF NF-L levels in male p25 mice. Spearman rank correlation analyses (n = 28) and Deming regression line in CA1 hippocampal area ($r = 0.788$, $p < 0.0001$), cortical layer II ($r = 0.741$, $p < 0.0001$), and cortical layer VI ($r = 0.817$, $p < 0.0001$). (B) Correlation between neuronal density (optical density of NeuN positive signal) and CSF NF-L levels in male p25 mice (n = 28). Spearman correlation and Deming regression line in CA1 hippocampal area ($r = -0.692$, $p < 0.0001$), cortical layer II ($r = -0.672$, $p < 0.0001$), and cortical layer VI ($r = -0.559$, $p = 0.0020$).

(2wON: 5874 ng/L, $p = 0.1453$ and 3wON: 20,828 ng/L, $p = 0.3778$). Altogether, these data indicate that switching off p25 expression prevented further increases in CSF NF-L levels. Repression of p25 expression also prevented further increases in serum NF-L levels between 2 and 5 weeks of induction (Fig. 2D). In this ON-OFF study, the serum NF-L levels correlated strongly with the CSF NF-L levels ($r = 0.794$, $p < 0.0001$; Fig. 2E).

3.3. Ongoing neurodegeneration and neuronal loss are stopped when p25 transgene is repressed

To evaluate ongoing neurodegeneration after p25 transgene expression, we quantified the number of Fluoro-Jade B-positive neurons in the hippocampus and in the cerebral cortical layers II and VI (Fig. 3A and C). No Fluoro-Jade B-positive cells were detected in control mice, whereas significant numbers of Fluoro-Jade B-positive neurons were present in all brain areas studied after p25 induction, in agreement with data obtained in another p25 inducible transgenic mouse model (Muyllaert et al., 2008). Staining appeared first in the DG hippocampal area and then in other hippocampal areas, CA1 and CA3, and cerebral cortex (data not shown). The number of Fluoro-Jade B-positive positive cells was higher in the hippocampus than in the cortex (Fig. 3A). In the CA1 hippocampal area and in the cortical layer II, the number of Fluoro-Jade B-positive cells significantly increased between 2 and 3wON ($p = 0.0006$ for CA1, and $p = 0.0001$ for cortex layer II), and remained stable between 3 and 5wON (Fig. 3A). By contrast, in the cortical layer VI (Fig. 3A), the number of Fluoro-Jade B-positive neurons increased between 2 and 3wON ($p < 0.0001$) and continued to increase between 3 and 5wON ($p = 0.0057$).

In the hippocampal CA1 area and in the cerebral cortical layers II and VI, switching off p25 transgene expression after 2wON (2wON + 3wOFF) stopped further increases in Fluoro-Jade B staining. Fluoro-Jade B staining in the 2wON + 3wOFF group was not significantly different from the 2wON group and was significantly lower ($p = 0.0350$) than the neurodegeneration measured at 5wON. There was no difference in Fluoro-Jade B staining when comparing the 3wON + 2wOFF group to the 3wON and 5wON groups, likely due to the fact that neurodegeneration process is stable in the CA1 area between 3 and 5 weeks. Similar results were obtained in the cerebral cortical layer II. However, in the cortical layer VI, although neurodegeneration progressively increased between 3 and 5wON, we failed to detect any difference between the 3wON + 2wOFF and the 5wON group, suggesting that it is difficult to stop the progression of neurodegeneration after 3 weeks of p25 induction in this model, or that a 2wOFF washout period is not long enough.

We next evaluated neuronal density by measuring NeuN immunostaining in the CA1 hippocampal area and in the cortical layers II and VI (Fig. 3B and D). Upon p25 induction, neuronal loss was observed in the CA1 hippocampal area between 2 and 5 weeks of transgene induction (−30%, $p = 0.0031$); neuronal density also appeared reduced in the cortical layers II and VI (−28%, $p = 0.0580$ and −25%, not significantly different from control period 2wON, respectively) (Fig. 3B). When p25 expression was switched off after 2wON (2wON + 3wOFF), neuronal staining intensity in the CA1 hippocampal area and in the cortical layer VI remained similar to the neuronal staining measured at the onset of p25 transgene repression, i.e., 2wON, and

higher than the neuronal staining at 5wON ($p = 0.0086$ and $p = 0.0423$ respectively), suggesting that neuronal loss was stopped. These data demonstrate that switching off p25 transgene prevents further neurodegeneration and neuronal loss in the CA1 hippocampal area and cerebral cortex.

3.4. CSF and serum NF-L levels correlate with neuronal damage in p25 mice

We further evaluated whether CSF NF-L levels were correlated with neuronal damage, i.e., ongoing neurodegeneration and neuronal loss in p25 mice. In the CA1 hippocampal area and cortical layers II and VI, CSF NF-L levels were significantly ($p < 0.0001$) and strongly correlated with ongoing neurodegeneration ($r = 0.788$, $r = 0.741$ and $r = 0.817$, respectively; Fig. 4A and Supplementary data, Table S1A). CSF NF-L levels were also significantly ($p < 0.0001$) and inversely correlated with neuronal density ($r = -0.692$, $r = -0.672$ and $r = -0.559$ in CA1 hippocampal area, cortical layers II and VI, respectively (Fig. 4B and Supplementary data, Table S1B). Statistically significant correlations were found between serum NF-L levels and ongoing neurodegeneration (Supplementary data, Table S1C) or neuronal loss (Supplementary data, Table S1D). In summary, CSF and serum NF-L levels appear to be correlated with neuronal damage in the brain of p25 mice.

3.5. CSF NF-L and serum NF-L can discriminate control from induced p25 mice

To evaluate whether CSF or plasma NF-L levels could discriminate between control and p25 mice we performed a receiver operating characteristic (ROC) analysis, an approach often used for biomarker validation studies in humans. Based on 65 control and 118 p25 mice, ROC curve analysis revealed that CSF and serum NF-L levels are able to discriminate control mice from p25 mice with an excellent area under the curve (AUROC = 1 and 0.97, respectively). For CSF ROC analysis (Fig. 5A), 2639 ng/L was determined as the optimal cut-off value and led to high sensitivity (0.991) and specificity (1). For serum ROC analysis, 100.54 ng/L was determined as the optimal cut-off value and led to a sensitivity of 0.983 and a specificity of 0.875 (Fig. 5B).

3.6. NF-L measured in CSF is not full-length NF-L

To characterize which form of NF-L is present in the CSF of p25 mice, we performed an SDS-PAGE analysis of immuno-captured NF-L. We first validated our Western blot antibody, a monoclonal antibody (C28E10) from Cell Signaling, on brain homogenates from control and p25 mice. We easily detected full length NF-L in brain which was not modulated upon p25 induction (data not shown).

Samples of recombinant bovine NF-L (ELISA standard, from 28 to 1000 pg) or CSF from p25 mice (300 pg NF-L as measured by ELISA) were then evaluated following immuno-capture on ELISA plates coated with a capture monoclonal NF-L antibody 47:3. The immuno-captured samples were evaluated by Western blot together with lysates from murine cerebral cortex (0.02 to 2 μg of total protein). Full-length NF-L (68 kDa) could be detected by Western blotting using the Cell Signaling antibody in the cerebral cortex of p25 mice and from immuno-captured recombinant bovine NF-L (up to 28 pg/well), but not in the CSF of p25 mice (Fig. 6A). No additional NF-L immuno-reactive band could be detected down to 20 kDa (Supplementary data, Fig. S3A). Similarly, no signal was detected in mice CSF using 2:1 antibody, with the exception of two immuno-reactive bands around 55 and 25 kDa, most probably corresponding to IgG heavy and light chain from 47:3 antibody used for immuno-capture (Supplementary data, Fig. S3B).

To determine whether NF-L was degraded in the CSF, we spiked CSF from control mice with 120 pg of full-length recombinant bovine NF-L and measured its expression by Western blot and by ELISA after different incubation times (0, 1, 6 or 24 h) at 37 °C. By Western blot the full-length NF-L signal decreased with incubation time and totally disappeared after 24 h. By contrast, when using an ELISA to detect NF-L there was only a 15% decrease of NF-L levels after incubating recombinant full-length NF-L in CSF for 24 h at 37 °C (Fig. 6B). Taken together, these data suggest that NF-L measured by ELISA in the CSF of p25 mice is probably not full-length NF-L. Based on the antibodies used in this study, the cleaved form of NF-L most likely lacks the epitope recognized by the Cell Signaling antibody (around amino-acid residue 455, according to supplier information), whereas it can be detected by the two antibodies used in the UmanDiagnostics NF-light® assay.

Similarly to our observations in p25 mice, high levels of CSF NF-L were also detected by ELISA in CSF from ThyTau22 mice, another

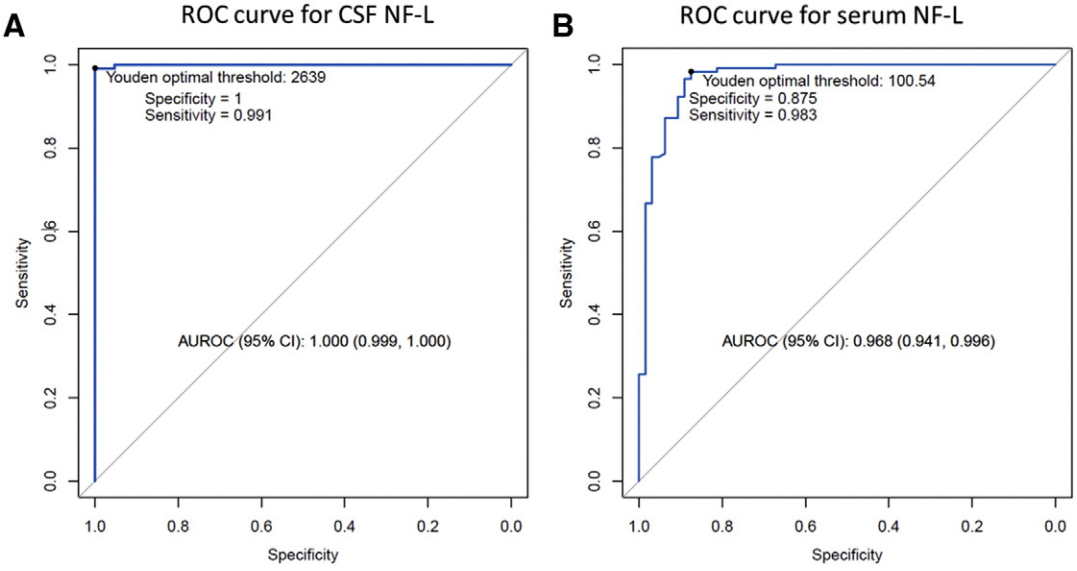

Fig. 5. CSF and serum NF-L can discriminate control from p25 mice. (A) Receiver operating curve (ROC) analysis for CSF NF-L in induced p25 mice and associated control mice ($n = 65$ Ctl mice + 118 p25 mice). The area under the ROC (AUROC) is equal to 1 (95% CI: [0.999–1.000]). For a calculated optimal threshold value (Youden's method) of 2639 ng/L, the sensitivity is equal to 0.991, and the specificity is equal to 1. (B) Receiver operating (ROC) analysis for serum NF-L in induced p25 mice and associated control mice ($n = 65$ Ctl mice + 118 p25 mice). The AUROC is equal to 0.968 (95% CI: [0.941–0.996]). For a calculated optimal threshold value (Youden's method) of 100.54 ng/L, the sensitivity is equal to 0.983, and the specificity is equal to 0.875.

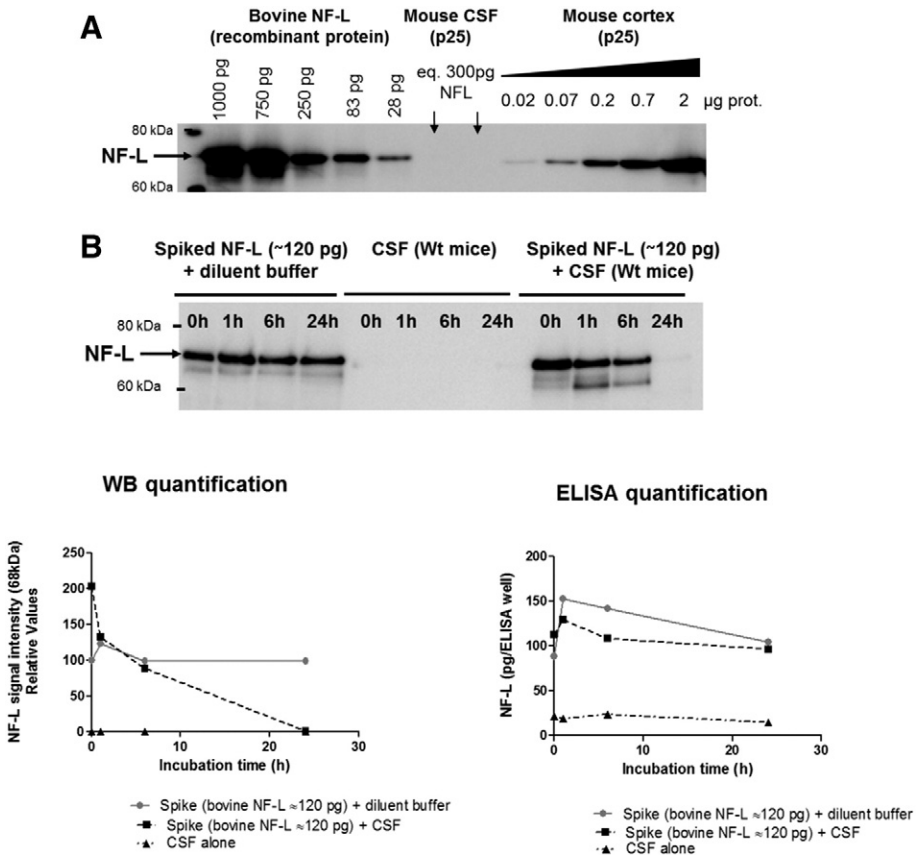

Fig. 6. Detection of CSF NF-L by Western blot and by ELISA kit. (A) Lack of detection of full-length NF-L by WB in CSF from p25 mice. Image of a Western blot membrane incubated with the primary anti NF-L antibody from Cell signaling (C28E10). The samples were first immuno-captured by incubation on UmanDiagnostics NF-light® ELISA plate before being denatured and loaded onto SDS-polyacrylamide gel. Three different samples were loaded: serial dilutions of recombinant bovine NF-L from the ELISA kit (1000 to 28 pg/WB well), two samples of CSF from p25 mice (corresponding to 300 pg NF-L loaded/WB well according to the concentration determined in parallel by ELISA), and serial dilutions of a lysate of p25 cerebral cortex (from 0.02 to 2 µg of total protein/WB well). NF-L (around 68 kDa) is detected by WB in recombinant bovine NF-L and mouse cortex samples but not in mouse CSF samples. (B) CSF from control mice or diluent buffer without CSF were spiked with 120 pg of recombinant bovine NF-L and NF-L was measured after different incubation times (0, 1, 6 or 24 h) at 37 °C by Western blotting using the Cell Signaling antibody (C28E10) or by ELISA. The top image shows the data obtained by Western blot and the graphs show quantification of NF-L levels by Western blot or by ELISA.

transgenic mouse model overexpressing human tau (Supplementary data, Fig. S4A), but full-length NF-L was not detected by Western blot with C28E10, the Cell Signaling anti-NF-L monoclonal antibody.

In order to better characterize which forms of NFL, full-length and/or truncated protein, are present in the CSF, we performed a mass spectrometry analysis of immuno-captured NF-L using 400 µL CSF from 9-month-old Thy-Tau22 mice (corresponding to 10 ng NF-L as measured by ELISA) (Supplementary methods). The immuno-captured sample was separated by SDS-PAGE and proteins were stained with Coomassie Blue dye (Supplementary data, Fig. S5A). The gel lane was then sliced into 9 bands below 85 kDa, which were digested with trypsin/LysC and the resulting peptide digest consecutively analysed by nanoLC-MS/MS as described in the Supplementary methods.

NF-L was identified with two tryptic peptides, Q341–K354 and E372–K380, only in the gel band 9 at around 10 kDa (Fig. S5B). No NF-L peptide was detected at the expected size for full-length NF-L (68 kDa). Peptide E372–K380 from NF-L is shared with Vimentin (P20152) and Desmin (P31001), two intermediate filament proteins also detected in the CSF sample but peptide Q341–K354 is found exclusively in NF-L, strongly suggesting that the fragment around 10 kDa in gel 9 belongs to NF-L.

Taken together, these data suggest that NF-L measured by ELISA in the CSF of Thy-Tau22 mice is not the full-length NF-L, but a cleaved form of the protein (approximately 10 kDa), which is nonetheless detected by the two antibodies used in the UmanDiagnostics NF-light® assay.

4. Discussion

In the present study, we used a model of inducible neurodegeneration, p25 mice, to evaluate whether NF-L levels in CSF or blood could be used as potential biomarkers of neurodegeneration. Our data demonstrate that increases in both CSF and serum NF-L levels are correlated with ongoing neurodegeneration and neuronal loss in the cerebral cortex and hippocampus and that both biomarkers can discriminate control from induced p25 mice. Moreover, when the expression of the p25 transgene is switched off, the levels of CSF NF-L do not increase further, mirroring the block of ongoing neurodegeneration and neuronal loss. The levels of CSF and serum NF-L are also correlated with the extent of neuronal damage suggesting that they could be used as dynamic biomarkers of neurodegeneration.

p25 mice are a rapid and aggressive model of neurodegeneration in brain regions where neuronal overexpression of human p25 transgene is induced (Cruz et al., 2003; Muyllaert et al., 2008). Previous studies have shown neurodegeneration, based on whole brain atrophy and decreases in hippocampal neuronal counts, starting after 6 weeks of p25 induction (Fischer et al., 2005), whereas our data, based on whole brain atrophy, Fluoro-Jade B staining and CSF NF-L, demonstrate that neurodegeneration can be detected as early as 3 weeks after p25 induction. By contrast, NeuN optical density in the hippocampus does not decrease before 5 weeks of p25 induction. We have also provided new data demonstrating that p25 transgene expression levels and CSF NF-L levels are higher in male than in female mice after p25 induction.

Although originally generated to explore the role of deregulated brain Cdk5 activity in triggering in vivo neurodegeneration, p25 mice display changes in several neurodegenerative mechanisms, including neuronal cytoskeletal alterations, abnormal protein hyperphosphorylation, synaptic dysfunction, cell cycle activation, DNA damage and activation of glial cells (Cruz et al., 2003; Fischer et al., 2005; Fischer et al., 2007; Kim et al., 2008; Sundaram et al., 2012). The ability to regulate the neurodegeneration phenotype in p25 mice makes this a relevant model to evaluate candidate dynamic biomarkers of neurodegenerative processes in biofluids.

In the ON-OFF study in p25 mice the increase in CSF NF-L levels more closely correlates with the increase in Fluoro-Jade B staining than with the decrease in neuronal density, indicating that CSF NF-L could be a more sensitive biomarker of a dynamic process of neurodegeneration rather than of neuronal loss. The absence of a decrease in CSF NF-L and Fluoro-Jade B staining during the short OFF period (2 or 3 weeks) could be due to a lag time between turning off transgene expression and stopping the ongoing neurodegenerative process. We did not detect any change in full-length NF-L levels when measured by Western Blot in the hippocampus from p25 mice which could be due to a lack of sensitivity by analysing a whole homogenate.

Very high levels of CSF NF-L (25,000 ng/L) are observed after only 4 weeks of transgene induction in male p25 mice. Such high levels of CSF NF-L have also been reported in three transgenic mouse models with different proteinopathy brain lesions, including α-synuclein A30P-αS, Tau P301S and APP/PS1 mice (Bacioglu et al., 2016). In TauP301S mice, CSF NF-L reached 40,000 ng/L in 10 to 12-month-old mice and reached 13,000 ng/L in 18-month-old APPPS1 mice. We have generated similar data in comparable transgenic mouse models, i.e., ThyTau22 mice, APP/PS1 and APP mice (see Supplementary data in Fig. S4). Bacioglu et al. (2016) also demonstrated in APP/PS1 mice that a BACE-1 inhibitor administered for six months (from 1.5 to 7.5 months) was able to reduce the increase of CSF NF-L, reinforcing the view that CSF NF-L may serve as a disease progression and pharmacodynamic biomarker in preclinical mouse models.

In humans, an increase in CSF NF-L has been associated with several CNS diseases. The highest increase in CSF NF-L levels has been described after an acute ischemic stroke (19,000 ng/L in patients with severe stroke) (Hjalmarsson et al., 2014). CSF-NF-L has also been used to stratify patients with ALS by showing that high concentrations of CSF NF-L (>5,000 ng/L) significantly correlated with disease progression and is a possible early indicator of the overall survival time (Tortelli et al., 2015). NF-L is also increased in CSF from FTD patients (6,762 ng/L in symptomatic FTD versus 650 ng/L in control) and the level of NF-L correlates with disease severity and brain atrophy measured by MRI (Meeter et al., 2016).

In AD and PD, CSF NF-L levels are lower than in FTD (Scherling et al., 2014). In a large cohort study, Skillbäck et al. (2013) showed that AD biomarker-positive subjects have higher NF-L levels, probably linked to cerebrovascular or subcortical axonal degeneration, but that it was more difficult to distinguish AD patients from controls >65 years old since CSF NF-L levels also increased with age (Skillbäck et al., 2014; Skillbäck et al., 2013). More recently, Zetterberg et al. (2016) showed that CSF NF-L concentrations correlated with accelerated cognitive decline in MCI patients and suggested that high CSF NF-L in AD or MCI could be an indicator of risk of rapid disease progression.

CSF NF-L levels have also been shown to be decreased during immuno-modulatory treatment in both RRMS and progressive MS patients. In RRMS, treatment with fingolimod decreased NF-L levels compared with placebo and reductions in NF-L correlated with an improvment in relapse and magnetic resonance imaging outcomes (Kuhle et al., 2015a). Natalizumab treatment in progressive MS patients also decreased CSF NF-L levels which was correlated with increases in the magnetization transfer ratio in both cortical grey and normal appearing white matter and EDSS improvement (Romme Christensen et al., 2014). Taken together, both the literature data and our results suggest that CSF NF-L could be used as a translational biomarker to following disease progression, neurodegeneration, and treatment efficacy in human neurodegenerative diseases.

Despite the high levels of CSF NF-L measured with the UmanDiagnostics NF-light® assay, we were not able to detect full length CSF NF-L by Western blot using the Cell Signaling anti-NF-L monoclonal antibody, C28E10. This is unlikely to be due to a lack of sensitivity with Western blot detection since the CSF NF-L loaded onto the gel was in the range of detection by Western blot and C28E10 was able to detect murine NF-L from the cerebral cortex of p25 mice. Furthermore, when recombinant NF-L was added to CSF and incubated for 24 h at 37 °C, the signal detected by Western blot totally disappeared. By contrast, the evaluation of NF-L concentrations by ELISA only revealed a 15% decrease compared to the starting concentration. This modest decrease is in accordance with the 13% decrease reported by Gunnarsson et al. (2011) (reply to Koel-Simmelink et al., 2011) after 24 h incubation of CSF NF-L at 37 °C.

The detection antibody used in the UmanDiagnostics NF-light® ELISA assay targets the central rod domain of NF-L, corresponding to an epitope which is different from the epitope recognized by C28E10 (in the tail domain, epitope around residue Glu450). Therefore, one possible explanation for the lack of detection of full length NF-L in CSF by Western blot is that CSF NF-L is cleaved in the tail domain and not detectable by C28E10, but can still be detected by ELISA. The mass spectrometry analysis of immuno-captured NF-L shows that at least in ThyTau22 mice, NF-L is detected in CSF as a cleaved form of the protein, of approximately 10 kDa, containing two tryptic peptides, Q341-K354 and E372-K380, the first one being found exclusively in the peptidic sequence of NF-L. In the CSF, the presence of cleaved protein forms has already been documented for Tau (Meredith et al., 2013) and neurogranin (Kvartsberg et al., 2015).

The classical ELISA assay used in our study has been described to be not sensitive enough to detect NF-L in human blood, leading to the development of a new ELISA format, based on electro-chemiluminescence detection (ECL) (Gaiottino et al., 2013; Kuhle et al., 2015b). With this ECL format, increased NF-L levels were reported in sera from RRMS patients (around 10 ng/L) (Disanto et al., 2016; Kuhle et al., 2016) and from FTD patients (around 31.5 ng/L in FTD versus 2.9 ng/L in controls) (Meeter et al., 2016). In both cases, serum and CSF NF-L levels were highly correlated. The UmanDiagnostics NF-L ELISA kit has also been transferred to the ultrasensitive SIMOA platform and used in a small pilot study in PSP patients to show that blood NF-L levels can discriminate PSP patients (31 ng/L) from control subjects (17.5 ng/L) (Rojas et al., 2016). Using the same approach, Rohrer et al. (2016) reported high blood NF-L levels in FTD patients (77 ng/L) compared to controls (19 ng/L).

In p25 mice, probably due to the very high levels of NF-L in CSF, we were able to detect NF-L in serum using the conventional NF-L ELISA format (lower detection limit of NF-L with UmanDiagnostics NF-light® assay is 31 ng/L). However, serum NF-L levels were 20 to 76-fold lower than CSF NF-L levels. Bacioglu et al. (2016) have reported CSF/plasma NF-L ratios of 30–70 in patients with neurodegenerative disorders (MSA, DLB, PSP, CBS, AD and MCI) and ratios of 30–40 in transgenic mice with different proteinopathy brain lesions, including α-synuclein A30P-αS, Tau P301S and APP/PS1 mice), ranges in good agreement with our data. The strong correlation between CSF NF-L and neuronal damage in the brain (Table S1), together with the fact that serum levels were 20 to 76-fold lower than CSF levels suggest that, in p25 mice, most of the NF-L in the blood originates from the CNS. Our ROC analyses also validate CSF NF-L and serum NF-L as relevant biomarkers, able to discriminate "non-neurodegenerative" control mice from "neurodegenerative" p25 mice and demonstrate that NF-L could be a relevant marker of the progressive and rapid neurodegeneration in this preclinical model.

In conclusion, we have shown that CSF and serum NF-L can be used as a biomarker of neurodegeneration in p25 mice. Our data provide additional evidence that CSF and serum NF-L levels are of interest to be further evaluated as both potential translational dynamic biomarkers

of neurodegeneration and as pharmacodynamic biomarkers to evaluate the efficacy of new neuroprotective agents in preclinical animal models and in clinical studies.

Conflict of interest statement

All authors were employees of Sanofi when the work was performed with the exception of Catherine Pech (Evotec).

Acknowledgments

We would like to thank Li Huei Tsai (Massachusetts Institute of Technology) for providing access to CamKII-TetOp25 mice and Niklas Norgren (UmanDiagnostics) for the gracious gift of 2:1 antibody. At Sanofi, we also thank Luc Esserméant and Dorothée Tamarelle for statistical analyses, Julie Durand and Patrick Juvet for technical assistance during the in vivo phase and a special thanks to Isabel A. Lefevre for critical reading of the manuscript. We finally wish to thank Marie Guillemot and François Autelitano (Evotec) for technical support and assistance in the NanoLC-MS/MS analysis.

Appendix A. Supplementary data

Supplementary data to this article can be found online at http://dx.doi.org/10.1016/j.nbd.2017.04.007.

References

Bacioglu, M., et al., 2016. Neurofilament light chain in blood and CSF as marker of disease progression in mouse models and in neurodegenerative diseases. Neuron 91, 494–496.
Bancher, C., et al., 1989. An antigenic profile of Lewy bodies: immunocytochemical indication for protein phosphorylation and ubiquitination. J. Neuropathol. Exp. Neurol. 48, 81–93.
Constantinescu, R., et al., 2009. Levels of the light subunit of neurofilament triplet protein in cerebrospinal fluid in Huntington's disease. Parkinsonism Relat. Disord. 15, 245–248.
Constantinescu, R., et al., 2010. Consecutive analyses of cerebrospinal fluid axonal and glial markers in Parkinson's disease and atypical parkinsonian disorders. Parkinsonism Relat. Disord. 16, 142–145.
Corbo, M., Hays, A.P., 1992. Peripherin and neurofilament protein coexist in spinal spheroids of motor neuron disease. J. Neuropathol. Exp. Neurol. 51, 531–537.
Cruz, J.C., et al., 2003. Aberrant Cdk5 activation by p25 triggers pathological events leading to neurodegeneration and neurofibrillary tangles. Neuron 40, 471–483.
DeMattos, R.B., et al., 2002. Plaque-associated disruption of CSF and plasma amyloid-beta (Abeta) equilibrium in a mouse model of Alzheimer's disease. J. Neurochem. 81, 229–236.
Disanto, G., et al., 2015. Serum neurofilament light chain levels are increased in patients with a clinically isolated syndrome. J. Neurol. Neurosurg. Psychiatry.
Disanto, G., et al., 2016. Serum neurofilament light chain levels are increased in patients with a clinically isolated syndrome. J. Neurol. Neurosurg. Psychiatry 87, 126–129.
Fischer, A., et al., 2005. Opposing roles of transient and prolonged expression of p25 in synaptic plasticity and hippocampus-dependent memory. Neuron 48, 825–838.
Fischer, A., et al., 2007. Recovery of learning and memory is associated with chromatin remodelling. Nature 447, 178–182.
Gaiottino, J., et al., 2013. Increased neurofilament light chain blood levels in neurodegenerative neurological diseases. PLoS One 8, e75091.
Giovannoni, G., Nath, A., 2011. After the storm: neurofilament levels as a surrogate endpoint for neuroaxonal damage. Neurology 76, 1200–1201.
Gunnarsson, M., et al., 2011. Axonal damage in relapsing multiple sclerosis is markedly reduced by natalizumab. Ann. Neurol. 69, 83–89.
Hall, S., et al., 2012. Accuracy of a panel of 5 cerebrospinal fluid biomarkers in the differential diagnosis of patients with dementia and/or parkinsonian disorders. Arch. Neurol. 69, 1445–1452.
Hansson, O., et al., 2017. Blood-based NfL: a biomarker for differential diagnosis of parkinsonian disorder. Neurology 88, 930–937.
Herbert, M.K., et al., 2015. CSF Neurofilament light chain but not FLT3 ligand discriminates parkinsonian disorders. Front. Neurol. 6, article 91.
Hill, W.D., et al., 1993. Neurofilament mRNA is reduced in Parkinson's disease substantia nigra pars compacta neurons. J. Comp. Neurol. 329, 328–336.
Hirano, A., 1991. Cytopathology of amyotrophic lateral sclerosis. Adv. Neurol. 56, 91–101.
Hjalmarsson, C., et al., 2014. Neuronal and glia-related biomarkers in cerebrospinal fluid of patients with acute ischemic stroke. J. Cent. Nerv. Syst. Dis. 6, 51–58.
Hoffman, P.N., et al., 1987. Neurofilament gene expression: a major determinant of axonal caliber. Proc. Natl. Acad. Sci. U. S. A. 84, 3472–3476.
Holmberg, B., et al., 1998. Increased cerebrospinal fluid levels of neurofilament protein in progressive supranuclear palsy and multiple-system atrophy compared with Parkinson's disease. Mov. Disord. 13, 70–77.
Hursh, J.B., 1939. Conduction velocity and diameter of nerve fibers. Am. J. Phys. 127, 131–139.
Kim, D., et al., 2008. Deregulation of HDAC1 by p25/Cdk5 in neurotoxicity. Neuron 60, 803–817.
Kim, K.K., et al., 2009. Identification of neuronal nuclei (NeuN) as Fox-3, a new member of the Fox-1 gene family of splicing factors. J. Biol. Chem. 284, 31052–31061.
Koel-Simmelink, M.J., et al., 2011. The neurofilament light chain is not stable in vitro. Ann. Neurol. 69, 1065–1066 (author reply 1066-7).
Kriz, J., et al., 2000. Electrophysiological properties of axons in mice lacking neurofilament subunit genes: disparity between conduction velocity and axon diameter in absence of NF-H. Brain Res. 885, 32–44.
Kuhle, J., et al., 2013. Neurofilament light and heavy subunits compared as therapeutic biomarkers in multiple sclerosis. Acta Neurol. Scand. 128, e33–e36.
Kuhle, J., et al., 2015a. Fingolimod and CSF neurofilament light chain levels in relapsing-remitting multiple sclerosis. Neurology 84, 1639–1643.
Kuhle, J., et al., 2015b. Serum neurofilament light chain is a biomarker of human spinal cord injury severity and outcome. J. Neurol. Neurosurg. Psychiatry 86, 273–279.
Kuhle, J., et al., 2016. Serum neurofilament light chain in early relapsing remitting MS is increased and correlates with CSF levels and with MRI measures of disease severity. Mult. Scler. 22, 1550–1559.
Kvartsberg, H., et al., 2015. Cerebrospinal fluid levels of the synaptic protein neurogranin correlates with cognitive decline in prodromal Alzheimer's disease. Alzheimers Dement. 11, 1180–1190.
Landqvist Waldo, M., et al., 2013. Cerebrospinal fluid neurofilament light chain protein levels in subtypes of frontotemporal dementia. BMC Neurol. 13, 54.
Leigh, P.N., et al., 1989. New aspects of the pathology of neurodegenerative disorders as revealed by ubiquitin antibodies. Acta Neuropathol. 79, 61–72.
Limberg, M., et al., 2016. Neurofilament light chain determination from peripheral blood samples. Methods Mol. Biol. 1304, 93–98.
Lu, C.H., et al., 2015. Neurofilament light chain: a prognostic biomarker in amyotrophic lateral sclerosis. Neurology 84, 2247–2257.
Lycke, J.N., et al., 1998. Neurofilament protein in cerebrospinal fluid: a potential marker of activity in multiple sclerosis. J. Neurol. Neurosurg. Psychiatry 64, 402–404.
Malmestrom, C., et al., 2003. Neurofilament light protein and glial fibrillary acidic protein as biological markers in MS. Neurology 61, 1720–1725.
Meeter, L.H., et al., 2016. Neurofilament light chain: a biomarker for genetic frontotemporal dementia. Ann. Clin. Transl. Neurol. 3, 623–636.
Meredith Jr., J.E., et al., 2013. Characterization of novel CSF Tau and ptau biomarkers for Alzheimer's disease. PLoS One 8, e76523.
Miyasaka, H., et al., 1993. Interaction of the tail domain of high molecular weight subunits of neurofilaments with the COOH-terminal region of tubulin and its regulation by tau protein kinase II. J. Biol. Chem. 268, 22695–22702.
Muyllaert, D., et al., 2008. Neurodegeneration and neuroinflammation in cdk5/p25-inducible mice: a model for hippocampal sclerosis and neocortical degeneration. Am. J. Pathol. 172, 470–485.
Norgren, N., et al., 2002. Monoclonal antibodies selective for low molecular weight neurofilaments. Hybrid Hybridomics. 21, 53–59.
Norgren, N., et al., 2003. Elevated neurofilament levels in neurological diseases. Brain Res. 987, 25–31.
Norgren, N., et al., 2004. Neurofilament and glial fibrillary acidic protein in multiple sclerosis. Neurology 63, 1586–1590.
Robin, X., et al., 2011. pROC: an open-source package for R and S+ to analyze and compare ROC curves. BMC Bioinformatics. 12, 77.
Rohrer, J.D., et al., 2016. Serum neurofilament light chain protein is a measure of disease intensity in frontotemporal dementia. Neurology 87, 1329–1336.
Rojas, J.C., et al., 2016. Plasma neurofilament light chain predicts progression in progressive supranuclear palsy. Ann. Clin. Transl. Neurol. 3, 216–225.
Romme Christensen, J., et al., 2014. Natalizumab in progressive MS: results of an open-label, phase 2A, proof-of-concept trial. Neurology 82, 1499–1507.
Rosengren, L.E., et al., 1996. Patients with amyotrophic lateral sclerosis and other neurodegenerative diseases have increased levels of neurofilament protein in CSF. J. Neurochem. 67, 2013–2018.
Scherling, C.S., et al., 2014. Cerebrospinal fluid neurofilament concentration reflects disease severity in frontotemporal degeneration. Ann. Neurol. 75, 116–126.
Schmued, L.C., et al., 1997. Fluoro-Jade: a novel fluorochrome for the sensitive and reliable histochemical localization of neuronal degeneration. Brain Res. 751, 37–46.
Semra, Y.K., et al., 2002. Heightened intrathecal release of axonal cytoskeletal proteins in multiple sclerosis is associated with progressive disease and clinical disability. J. Neuroimmunol. 122, 132–139.
Skillbäck, T., et al., 2013. Cerebrospinal fluid biomarkers for Alzheimer disease and subcortical axonal damage in 5542 clinical samples. Alzheimers Res. Ther. 5, 47.
Skillbäck, T., et al., 2014. CSF neurofilament light differs in neurodegenerative diseases and predicts severity and survival. Neurology 83, 1945–1953.
Soelberg Sorensen, P., Sellebjerg, F., 2016. Neurofilament in CSF-A biomarker of disease activity and long-term prognosis in multiple sclerosis. Mult. Scler. 22, 1112–1113.
Sundaram, J.R., et al., 2012. Cdk5/p25-induced cytosolic PLA2-mediated lysophosphatidylcholine production regulates neuroinflammation and triggers neurodegeneration. J. Neurosci. 32, 1020–1034.
Tortelli, R., et al., 2015. Pseudobulbar affect (PBA) in an incident ALS cohort: results from the Apulia registry (SLAP). J. Neurol.
Wolf, H.K., et al., 1996. NeuN: a useful neuronal marker for diagnostic histopathology. J. Histochem. Cytochem. 44, 1167–1171.
Yuan, A., et al., 2012. Neurofilaments at a glance. J. Cell Sci. 125, 3257–3263.
Zetterberg, H., et al., 2016. Association of cerebrospinal fluid neurofilament light concentration with Alzheimer disease progression. JAMA Neurol. 73, 60–67.